# Supplemental Data

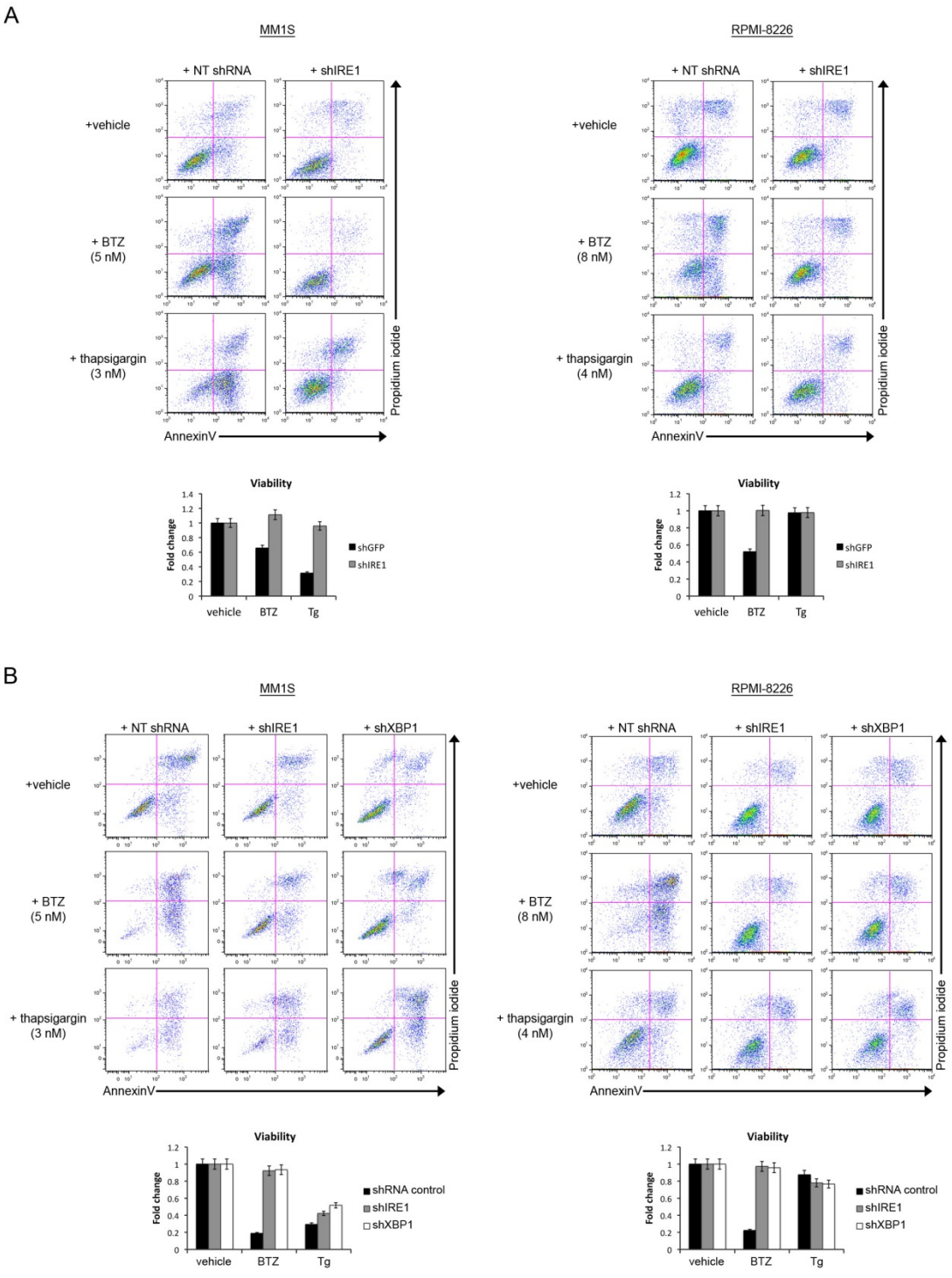

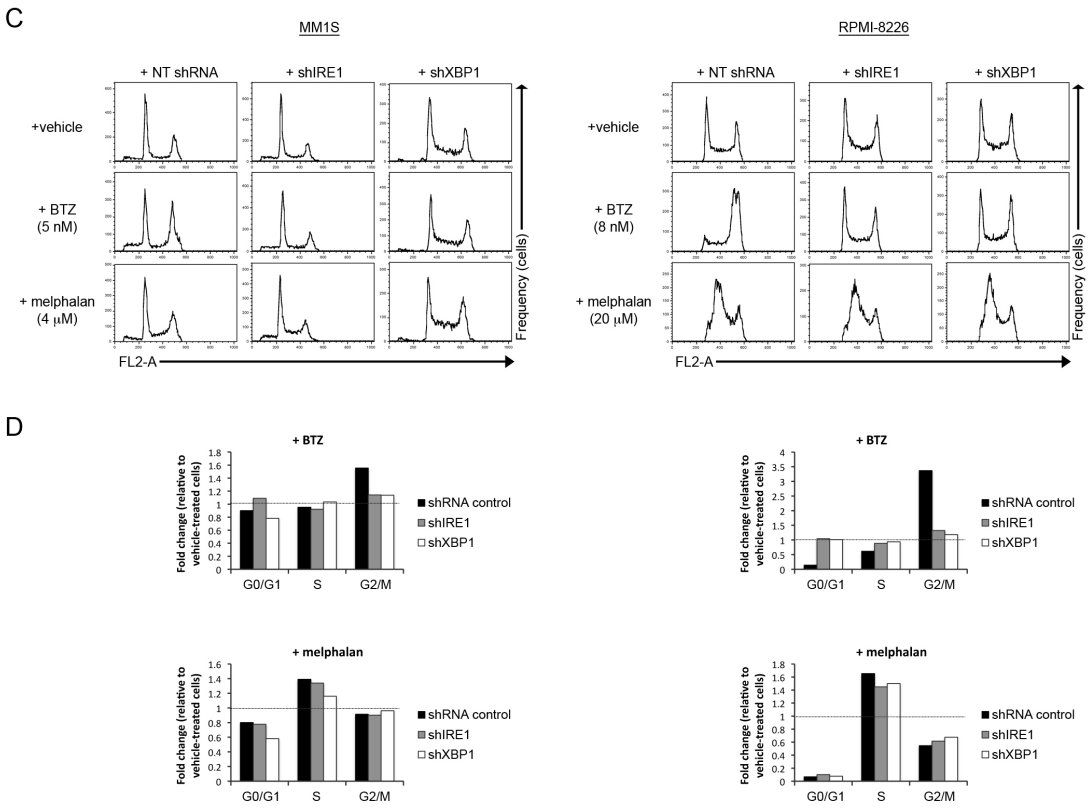


**Figure S1, related to Figure 1. Suppression of Ire1-Xbp1s protects MM cells from BTZ-induced apoptosis and cell cycle arrest. (A)** MM1S (left panels) and RPMI-8226 (right panels) MM cells were separately infected with lentivirus expressing either a control Non-Targeted (NT) shRNA or shIRE1 and grown for 48 hours; cells were then treated with BTZ or thapsigargin at the specified concentrations (approximately IC80) for a further 24 hours and apoptosis was assessed by AnnexinV-FITC and propidium iodide staining. The bar graphs below show fold-change in viable (Annexin $V^-$ $PI^-$) cells, following treatment with BTZ or thapsigargin (Tg), normalized to the viability of cells treated with vehicle alone. **(B)** Same as for (A) except that cells were first treated with shIRE1, shXBP1 or NT shRNA; and then treated with BTZ or Tg for 48 hours. **(C)** MM1S (left) and RPMI-8226 cells (right) expressing control shRNA, shIRE1 or shXBP1 were treated with BTZ or melphalan at the specified concentrations for 24 hours and cell cycle analyses were performed. **(D)** Fold-change in the percentage of MM1S (left) or RPMI-8226 (right) cells in G0/G1, S, or G2/M phases of cell cycle, following 24 hour exposure to BTZ or melphalan, normalized to the distribution of control cells treated with vehicle alone.

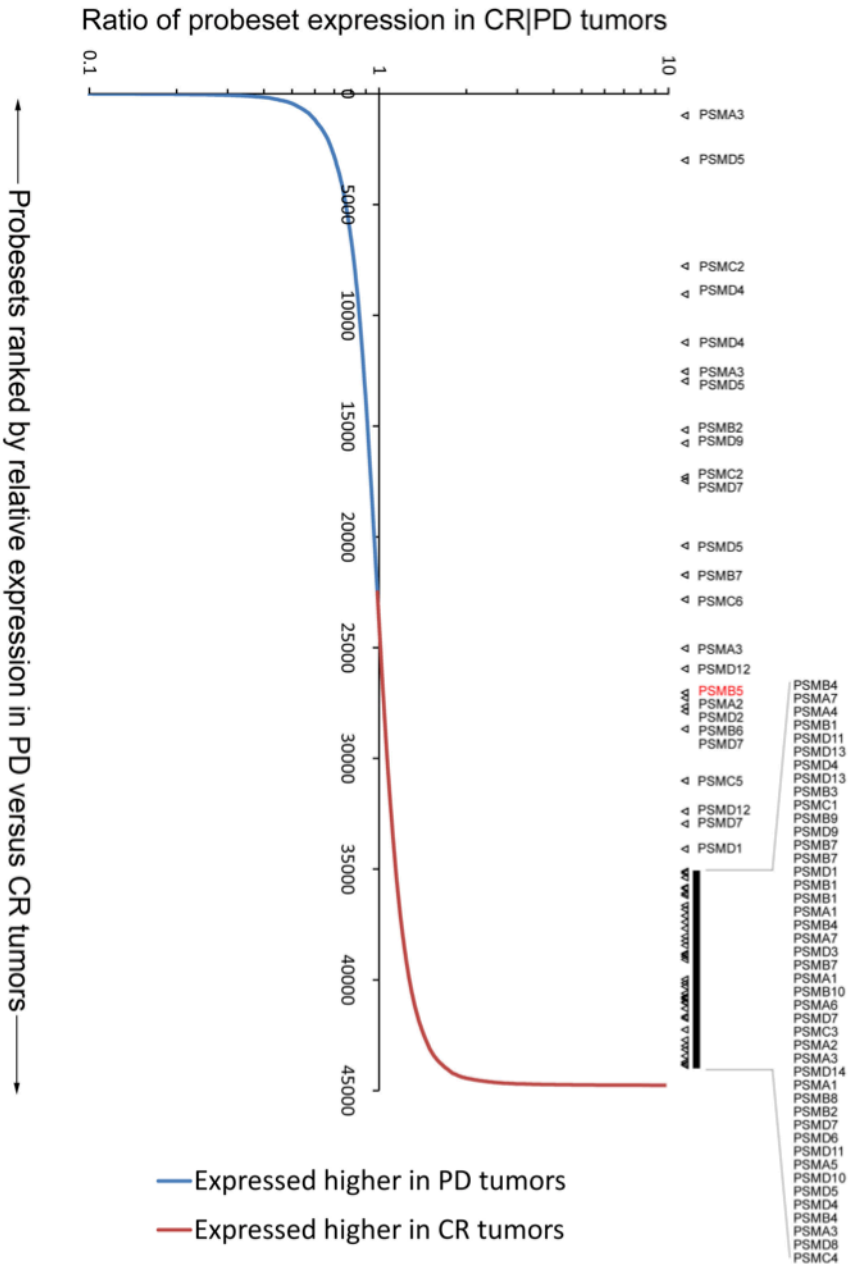


**Figure S2, related to Figure 2. The majority of proteasome subunits are expressed at lower levels in MM tumors that prove resistant to BTZ.** Gene expression analysis of primary tumor cells from MM patients, showing the ranked pre-treatment expression of 44760 probesets amongst tumors that showed either a complete response (CR) or progressive disease (PD) on clinical BTZ therapy. Probesets are plotted on the vertical axis by rank-order of relative expression in PD versus CR tumors. The ranking (differential expression) of proteasome (PSM) subunit probesets is shown to the right of the plot. PSMB5 is shown in red.

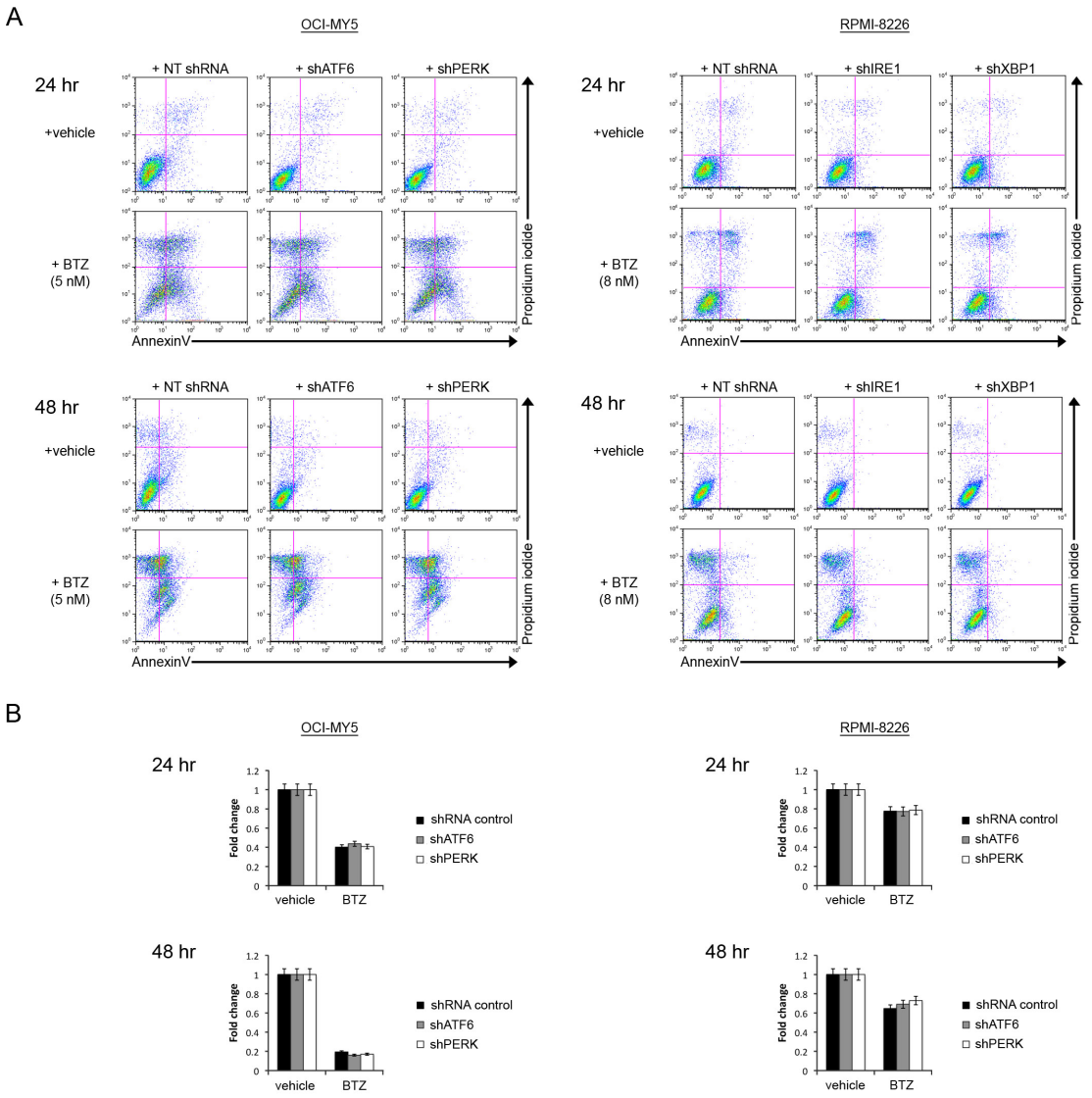


**Figure S3, related to Figure 3. shPERK and shATF6 have minimal effect on BTZ-induced MM cell apoptosis.** (A) OCI-MY5 (left) and RPMI-8226 (right) MM cells were infected with LV expressing non-targeted (NT) control shRNA, or shATF6 or shPERK, for 48 hours and then treated with BTZ at the indicated concentration. Apoptosis was assessed by Annexin V-PI flow cytometry at 24 (upper panels) and 48 hours (lower panels). (B) Fold-change in viable (Annexin V- PI-) OCI-MY5 (left) or RPMI-8226 (right) cells, following treatment with BTZ, normalized to the viability of cells treated with vehicle alone.

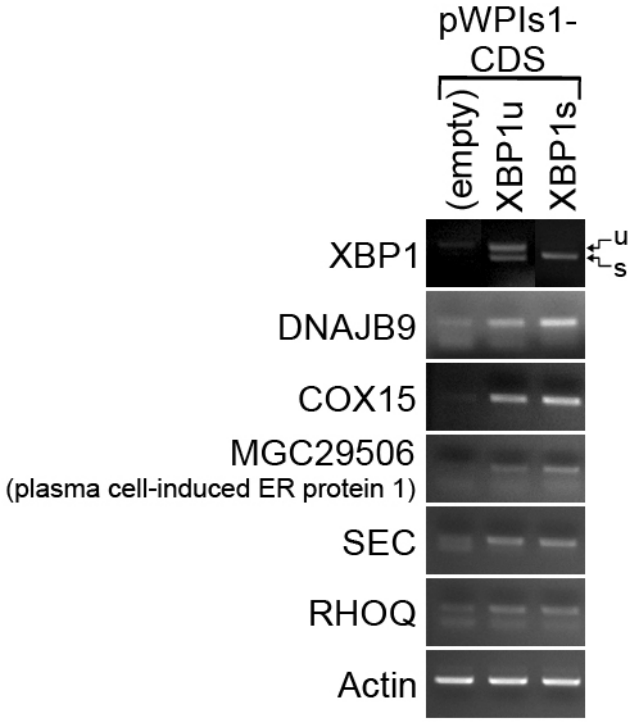


**Figure S4, related to Figure 4. Induction of Xbp1 target genes by ectopically expressed XBP1s cDNA.** OCI-MY5 MM cells expressing integrated lentiviral 3' UTR shXBP1, were infected with empty pWPIs1 vector (lane 1), or vector expressing XBP1u (lane 2) or XBP1s (lane 3) cDNA. Xbp1s target gene expression was assessed by semi-quantitative PCR. Note that expressed XBP1u mRNA was partially spliced to XBP1s, as shown.

A

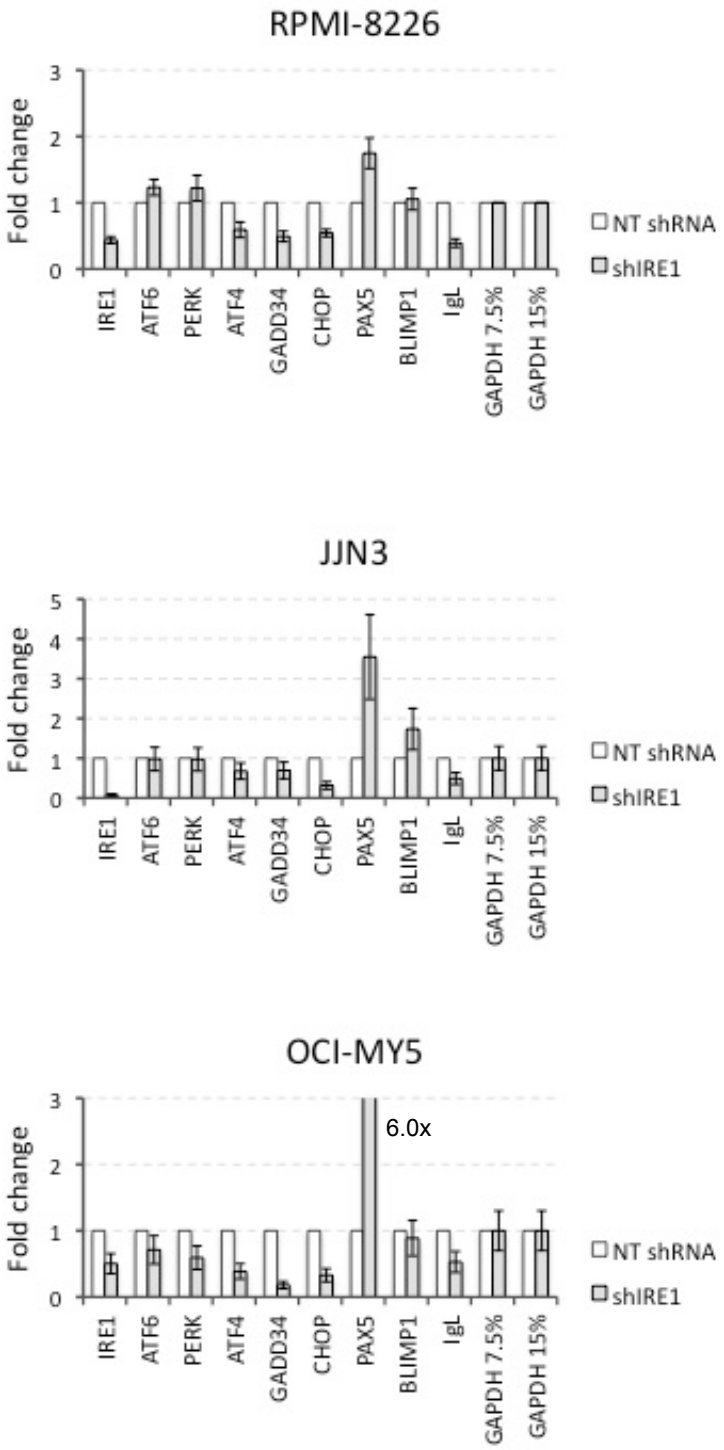
RPMI-8226
Fold change
3
2
1
0
IRE1
ATF6
PERK
ATF4
GADD34
CHOP
PAX5
BLIMP1
IgL
GAPDH 7.5%
GAPDH 15%
NT shRNA
shIRE1
JJN3
Fold change
5
4
3
2
1
0
IRE1
ATF6
PERK
ATF4
GADD34
CHOP
PAX5
BLIMP1
IgL
GAPDH 7.5%
GAPDH 15%
NT shRNA
shIRE1
OCI-MY5
Fold change
3
2
1
0
6.0x
IRE1
ATF6
PERK
ATF4
GADD34
CHOP
PAX5
BLIMP1
IgL
GAPDH 7.5%
GAPDH 15%
NT shRNA
shIRE1

B

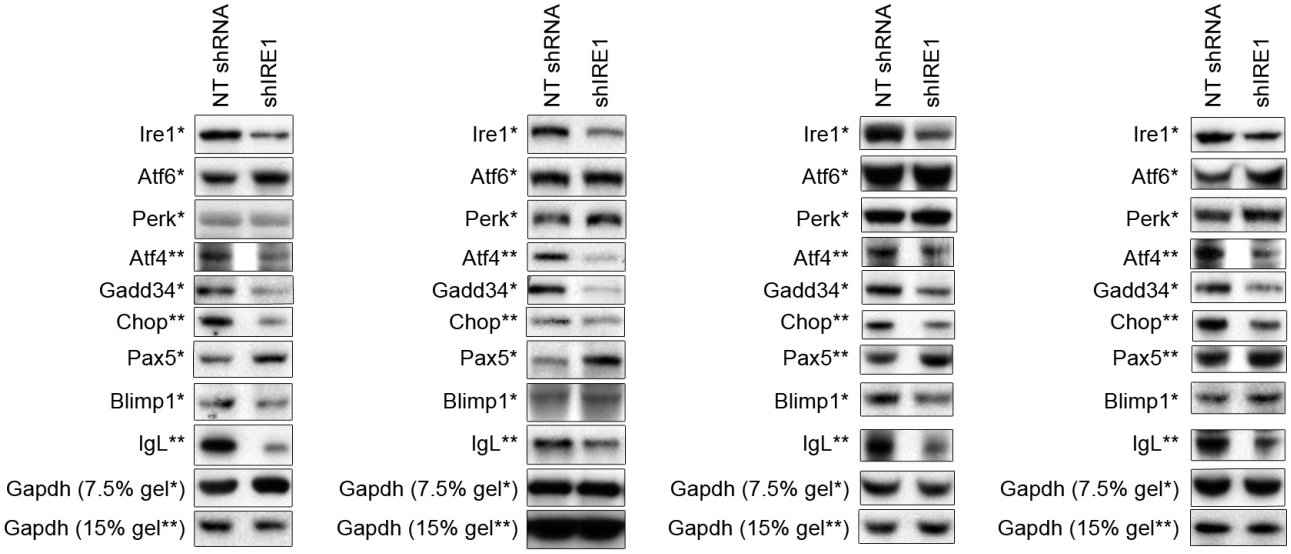
NT shRNA
shIRE1
Ire1*
Atf6*
Perk*
Atf4**
Gadd34*
Chop**
Pax5*
Blimp1*
IgL**
Gapdh (7.5% gel*)
Gapdh (15% gel**)
NT shRNA
shIRE1
Ire1*
Atf6*
Perk*
Atf4**
Gadd34*
Chop**
Pax5*
Blimp1*
IgL**
Gapdh (7.5% gel*)
Gapdh (15% gel**)
NT shRNA
shIRE1
Ire1*
Atf6*
Perk*
Atf4**
Gadd34*
Chop**
Pax5**
Blimp1*
IgL**
Gapdh (7.5% gel*)
Gapdh (15% gel**)
NT shRNA
shIRE1
Ire1*
Atf6*
Perk*
Atf4**
Gadd34*
Chop**
Pax5**
Blimp1*
IgL**
Gapdh (7.5% gel*)
Gapdh (15% gel**)

C

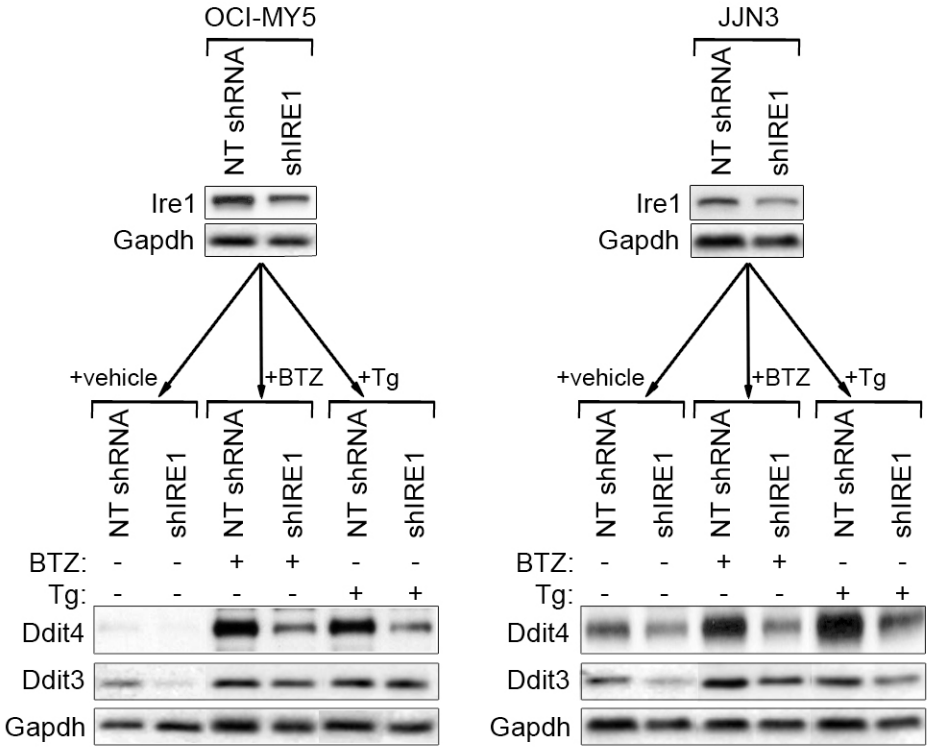
OCI-MY5
NT shRNA
shIRE1
Ire1
Gapdh
+vehicle
+BTZ
+Tg
NT shRNA
shIRE1
NT shRNA
shIRE1
NT shRNA
shIRE1
BTZ: - - + + - -
Tg: - - - - + +
Ddit4
Ddit3
Gapdh
JJN3
NT shRNA
shIRE1
Ire1
Gapdh
+vehicle
+BTZ
+Tg
NT shRNA
shIRE1
NT shRNA
shIRE1
NT shRNA
shIRE1
BTZ: - - + + - -
Tg: - - - - + +
Ddit4
Ddit3
Gapdh

D

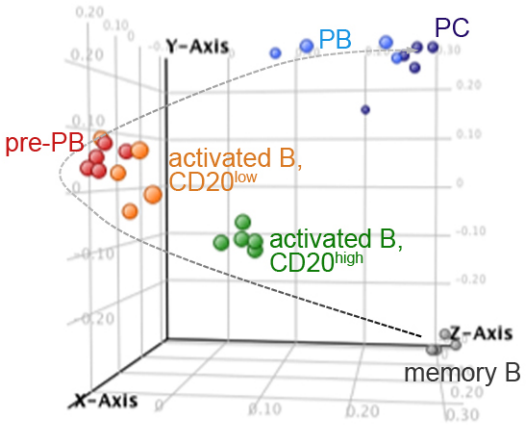
Y-Axis
PB
PC
pre-PB
activated B,
CD20low
activated B,
CD20high
Z-Axis
memory B
X-Axis

E

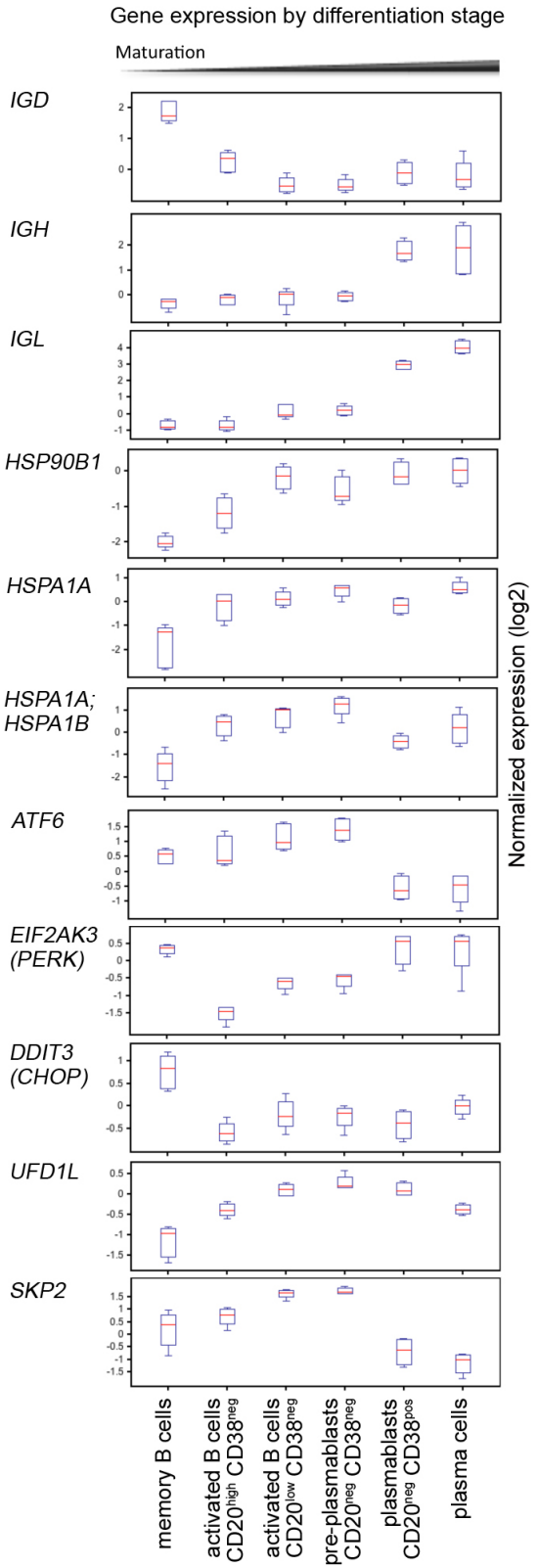
Gene expression by differentiation stage
Maturation
IGD
IGH
IGL
HSP90B1
HSPA1A
HSPA1A;
HSPA1B
ATF6
EIF2AK3
(PERK)
DDIT3
(CHOP)
UFD1L
SKP2
Normalized expression (log2)
memory B cells
activated B cells CD38neg CD20high
activated B cells CD38neg CD20low
pre-plasmablasts CD38neg CD20neg
plasmablasts CD38pos CD20neg
plasma cells

**Figure S5, related to Figure 5.** (A) The relative expression (fold-change) of indicated proteins in RPMI-8226, JJN3 and OCI-MY5 MM cells in Figure 5D, following Ire1 silencing. Immunoblot bands were quantified by image scanning densitometry and normalized to NT shRNA and GAPDH controls. RPMI-8226 values represent the mean of replicate experiments (n=4) and error bars show the SEM. OCI-MY5 and JJN3 values were calculated from densitometry assessments of single optimized experiments and error bars represent ± 30% error. OCI-MY5 expression of Pax5 was increased 6-fold following shIRE1 exposure. (B) Immunoblot detection of indicated proteins in RPMI-8226 cells expressing shIRE1. The results of four independent experiments are shown. (C) OCI-MY5 and JJN3 MM cells were infected with lentivirus to express NT shRNA or shIRE1 for 18 hr, washed and grown for a further 48 hr, divided and then treated with vehicle, BTZ 100nM or Tg 200nM for 6 hr. Knock down of Ire1 was confirmed on pre-treatment cells. The effect of Ire1 knockdown on Ddit3 (Chop) and Ddit4 (Redd1) induction by drug was assessed by immunoblot. *DDIT4* is an Atf4 target gene upregulated by ER stress (NCBI GEO Proflies GDS4089, GDS4090, GDS4130)(Jin et al., 2009) (Dombroski et al., 2010; Prenzel et al., 2011). (D) Principal component analysis of gene expression changes during the differentiation of memory B cells to plasma cells, showing that gene expression across these maturation stages is substantively U-shaped. Both principal component 1 (x-axis, accounting for 39.4% variation) and 3 (z-axis, accounting for 13.5% variation) show maximal deviation in gene expression from memory B cells at activated B cell and pre-plasmablast stages, which is reversed as these cells mature into plasma cells. (E) Box-whisker plots of relative mRNA expression of immunoglobulins (IGH, IGL, IGD), chaperones (HSP90B1, DNAJB9, HSPA1A, HSPA1B) and UPR genes (bottom panels) during B cell to plasma cell maturation, plotted on log(2) scale. UFD1L is repressed by ER stress, and acts to suppress SKP2, coupling ER stress to cell cycle delay (Chen et al., 2011).

**Table S1, related to Figure 5.** Gene Set Enrichment Analysis for plasma cell-lineage maturation gene set expression in MM tumors that respond to BTZ (with complete response) or that fail to respond to BTZ (with progressive disease)

GSEA: Genes expressed higher in myeloma tumors that responded to BTZ (APEX 039) versus plasma cell (PC) maturation gene sets

| Gene set | Total genes | Genes found | p-value | q-value | NES |
|---|---|---|---|---|---|
| UP>2-fold: [PCs] vs [memory B cells] | 5982 | 4181 | <0.001 | <0.001 | 1.654 |
| UP>2-fold: [PCs] vs [Activated D4 $CD20^{neg}$ $CD38^{neg}$ pre-plasmablasts] | 5076 | 3340 | 0.035 | 0.03 | 1.428 |
| UP>2-fold: [PCs] vs [Activated D4 $CD20^{high}$ $CD38^{neg}$ B cells] | 4972 | 3310 | 0.012 | 0.031 | 1.511 |
| UP>2-fold: [PCs] vs [Activated D4 $CD20^{low}$ $CD38^{neg}$ B cells] | 5055 | 3336 | 0.029 | 0.034 | 1.439 |
| UP>2-fold: [PCs] vs [Activated D7 $CD20^{neg}$ $CD38^{pos}$ plasmablasts] | 5318 | 3435 | 0.027 | 0.044 | 1.441 |

GSEA: Genes expressed higher in myeloma tumors that progressed on BTZ (APEX 039) versus plasma cell (PC) maturation gene sets

| Gene set | Total genes | Genes found | p-value | q-value | NES |
|---|---|---|---|---|---|
| UP>2-fold: [PCs] vs [Activated D7 $CD20^{neg}$ $CD38^{pos}$ plasmablasts] | 5318 | 3702 | <0.001 | 0.004 | -1.596 |
| UP>2-fold: [PCs] vs [Activated D4 $CD20^{high}$ $CD38^{neg}$ B cells] | 4972 | 3359 | 0.004 | 0.005 | -1.556 |
| UP>2-fold: [PCs] vs [memory B cells] | 5982 | 3769 | 0.006 | 0.008 | -1.49 |
| UP>2-fold: [PCs] vs [Activated D4 $CD20^{neg}$ $CD38^{neg}$ pre-plasmablasts] | 5076 | 3486 | 0.01 | 0.009 | -1.502 |
| UP>2-fold: [PCs] vs [Activated D4 $CD20^{low}$ $CD38^{neg}$ B cells] | 5055 | 3458 | 0.008 | 0.01 | -1.526 |

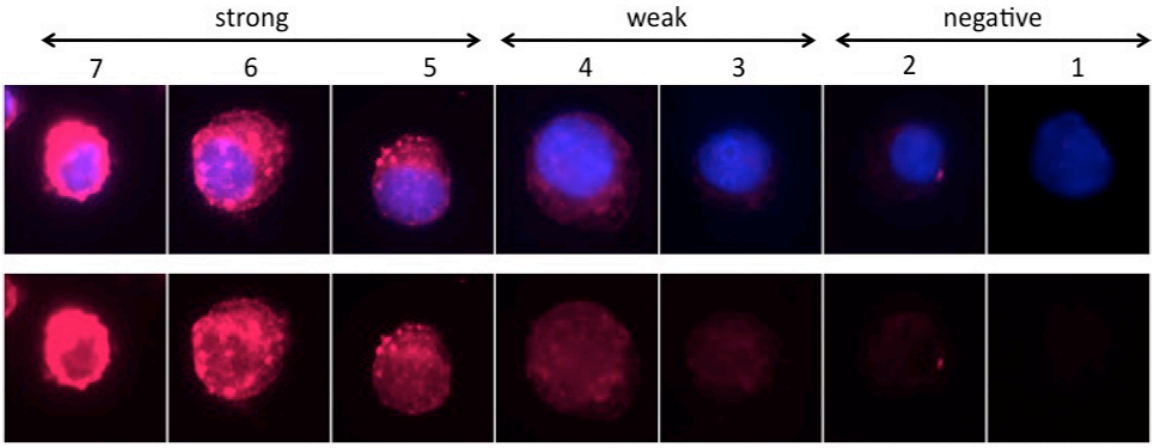


**Figure S6, related to Figure 6. Xbp1s IF Quantification Scale.** Scale used to categorize primary MM tumor cells for immunoflourescence-based Xbp1s expression. Cells were divided into Xbp1s positive (strong), weak, or negative categories.

A

a

| | |
|---|---|
| Patient | female, age 39 |
| Myeloma status | relapse (off treatment) |
| Last treatment(s) | CyBorD |
| Time since treatment | 2 months |
| FISH abnormality | del(1p32.3) |

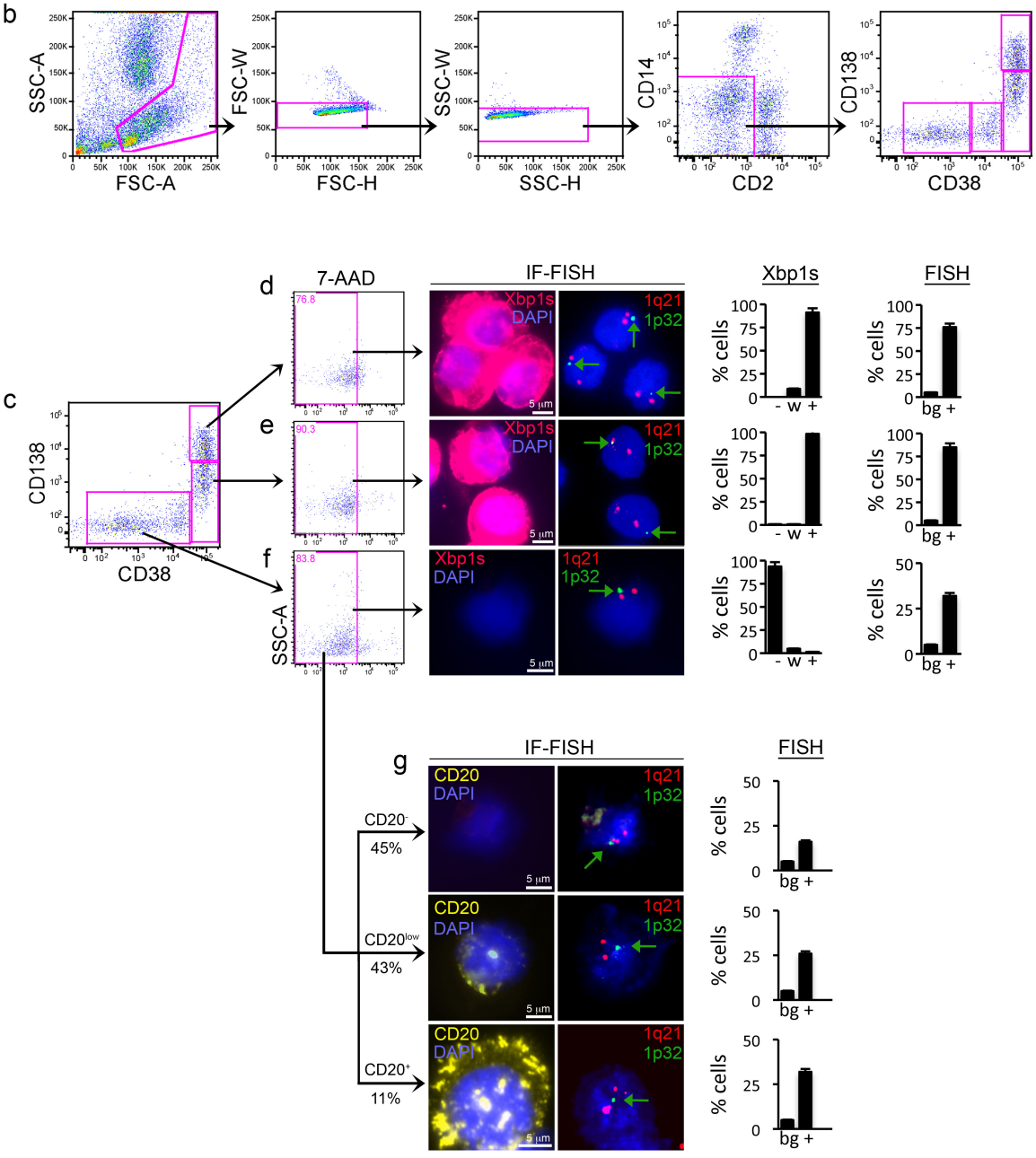

B

a

| | |
|---|---|
| Patient | male, age 50 |
| Myeloma status | PD (on CyBorD) |
| Last treatment(s) | CyBorD |
| Time since treatment | 7 days |
| FISH abnormality | Hyperdiploidy |

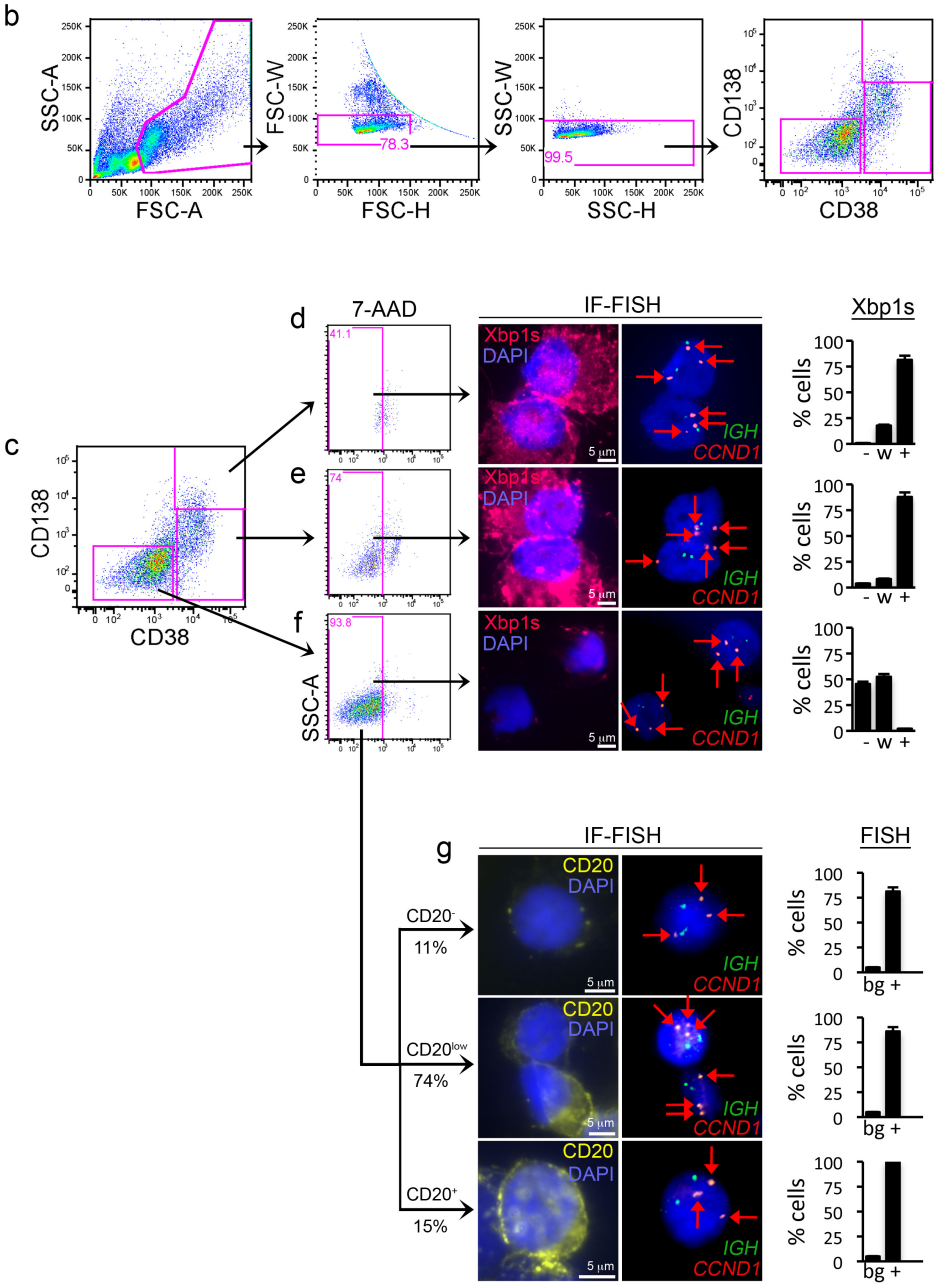

C

a

| | |
|---|---|
| Patient | male, age 48 |
| Myeloma status | minimal residual disease post treatment |
| Last treatment(s) | CyBorD + DPACEx2 |
| Time since treatment | 3 weeks |
| FISH abnormality | t(11;14) *IGH-CCND1* |

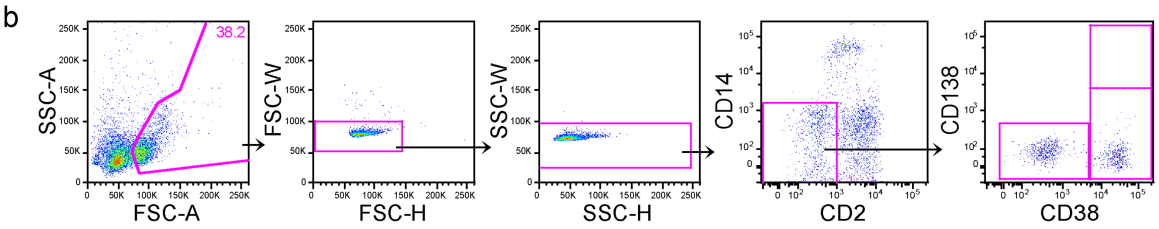


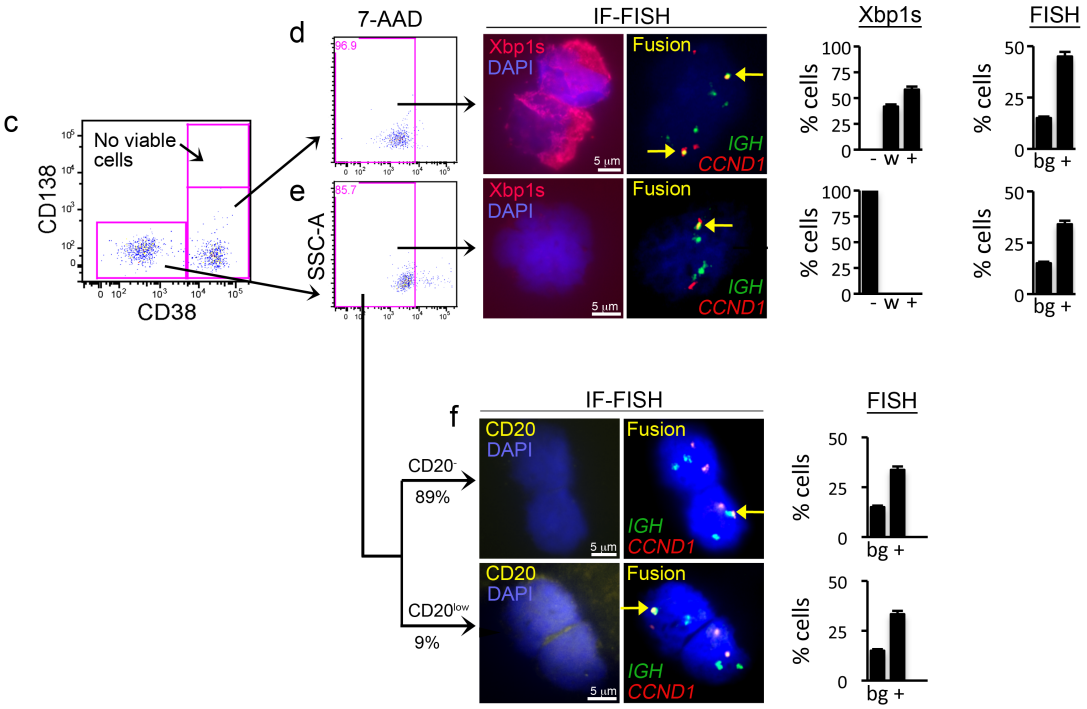

D

a

| | |
|---|---|
| Patient | female, age 55 |
| Myeloma status | PD (on dexamethasone) |
| Last treatment(s) | CyBorD, followed by dexamethasone maintenance |
| Time since treatment | 7 days |
| FISH abnormality | t(4;14) *IGH-FGFR3* |

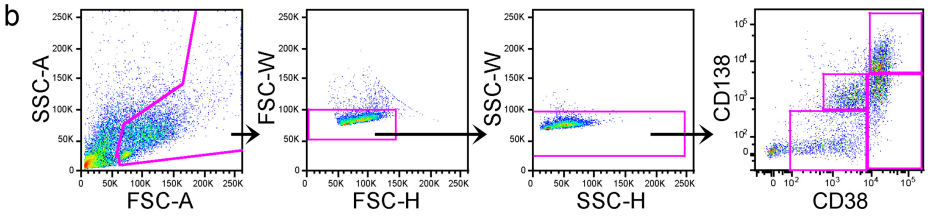


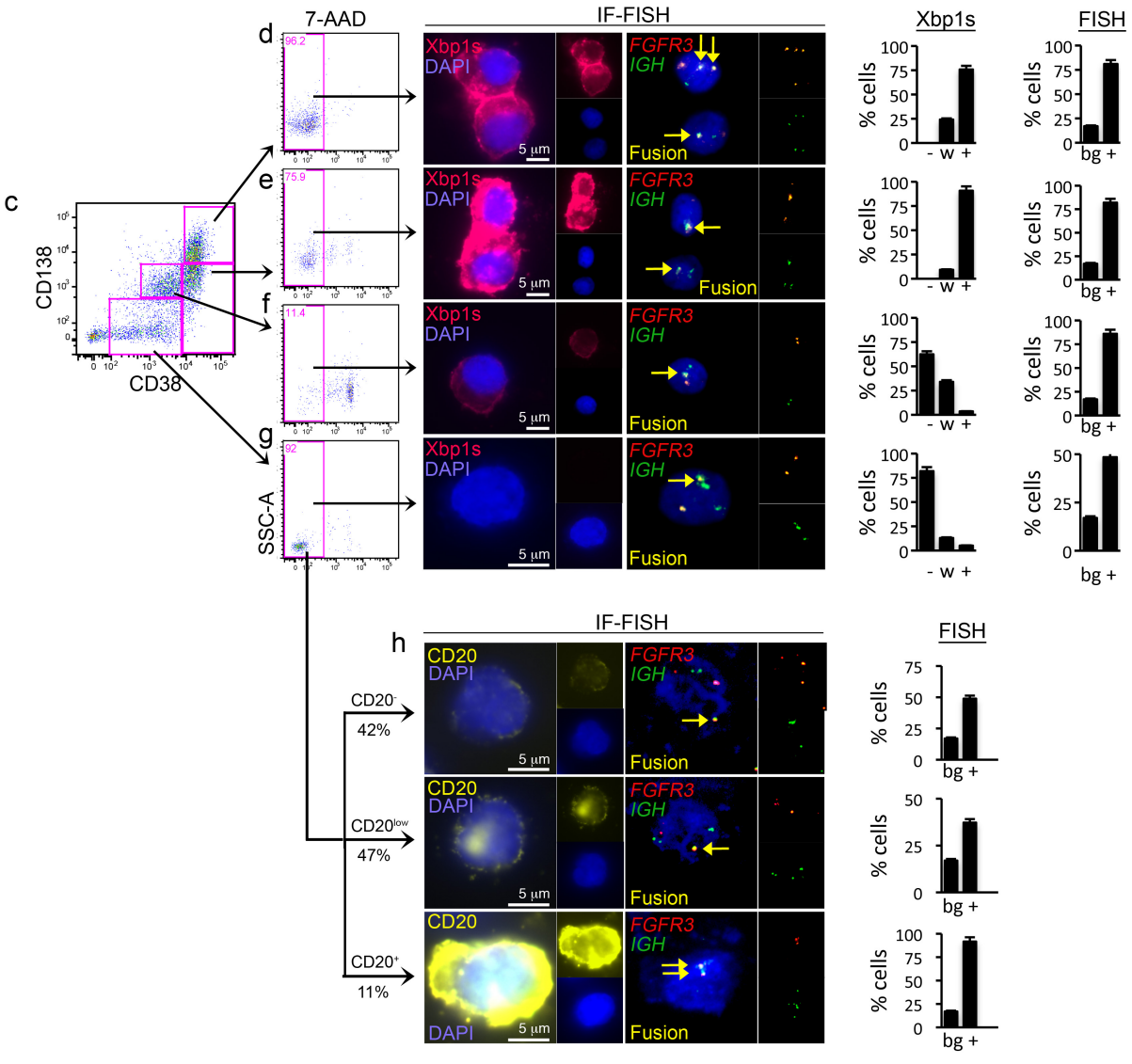

**Figure S7, related to Figure 7. Tumor Progenitor Subpopulations in MM patients.**

(A) Findings from a patient with relapsed MM following BTZ discontinuation. (a) The clinical information of the patient whose bone marrow was examined. (b) Bone marrow MM cells were enriched by sequential FACS for lymphoid FSC/SSC (left panel), by removal of aggregates (second and third panels) and by negative selection for CD2 (T and NK cells) and CD14 (monocytes). Gates are shown in pink. (c) Tumor cells gated into subpopulations by CD38 and CD138 status. Viable $CD38^{+}$ $CD138^{+}$ plasma cells (d), $CD38^{+}$ $CD138^{-/low}$ plasmablasts (e), and $CD38^{-}$ $CD138^{-}$ cells (f) were examined for the presence of Xbp1s protein and for the loss of chromosome 1p32 (green arrows), which contains the *CDKN2C* locus, by IF-FISH. Each row illustrates a single cell. Scale bars (5μm) are identical for IF and FISH. The overall proportion of cells in each subpopulation with strong (+), weak (w) or no (-) expression of Xbp1s and the proportion of cells positive (+) for loss of chromosome 1p32, compared with the background rate (bg), are quantified and shown in the bar graphs. (g) Viable $CD38^{-}$ $CD138^{-}$ B cells were also examined for CD20 expression and for chromosome 1p32 loss by IF-FISH.

(B) Findings from a MM patient with progression on BTZ therapy. (a) The clinical information of the patient. (b) Bone marrow MM cells were enriched by FACS for lymphoid FSC/SSC (left panel) and by removal of aggregates (second and third panels) and were gated into subpopulations by CD38 and CD138 status (c). Viable $CD38^{+}$ $CD138^{+}$ plasma cells (d), $CD38^{+}$ $CD138^{-/low}$ plasmablasts (e), and $CD38^{-}$ $CD138^{-}$ cells (f) were examined for the presence of Xbp1s and for trisomy of chromosome 11, which contains the *CCND1* locus (red arrows), by IF-FISH. Bar graphs show the overall proportion of cells with expression of Xbp1s and the proportion of cells positive for loss of chromosome 1p32, compared with the background rate. (g) Viable $CD38^{-}$ $CD138^{-}$ B cells were also examined for CD20 expression and for gain of *CCND1* by IF-FISH.

(C) Findings from a MM patient following intensive BTZ and DPACE chemotherapy with clinical response. (a) The clinical information of the patient. (b) The patient's bone marrow was FACS sorted as in (Ab) and MM cells were gated into subpopulations by CD38 and CD138 status (c). Viable $CD38^{+}$ $CD138^{+}$ plasma cells were not identified. Viable $CD38^{+}$ $CD138^{-/low}$ plasmablasts (d) and $CD38^{-}$ $CD138^{-}$ B cells (e) were examined for concurrent Xbp1s protein expression and for *IGH-CCND1* gene fusion (yellow arrows) by IF-FISH. Bar graphs show the overall proportion of cells with expression of Xbp1s and the proportion of cells positive for the *IGH-CCND1* gene fusion, compared

with the background rate. (f) Viable $CD38^-$ $CD138^-$ B cells were also examined for CD20 expression and for *IGH-CCND1* by IF-FISH.

(D) Findings from a patient with relapsed MM following BTZ discontinuation, on dexamethasone treatment. (a) The clinical information of the patient whose bone marrow was examined. (b) The patient's bone marrow was FACS sorted as in (Bb) and were gated into subpopulations by CD38 and CD138 status (c). Viable $CD38^+$ $CD138^+$ plasma cells (d), $CD38^+$ $CD138^{-/low}$ plasmablasts (e), and $CD38^-$ $CD138^-$ cells (g) were examined for the presence of Xbp1s and for *IGH-FGFR3* gene fusion (yellow arrows) by IF-FISH. A second plasma cell population, shedding CD38 and CD138 and largely nonviable (f), was also examined. (h) Viable $CD38^-$ $CD138^-$ B cells were also examined for CD20 expression and for *IGH-FGFR3* by IF-FISH. Scale bars (5μm) are identical for IF and FISH; monochrome insets are shown at 0.5x scale.

## SUPPLEMENTAL EXPERIMENTAL PROCEDURES

### Cell culture and constructs

Methods for MM cell culture, production of shRNA or cDNA expressing lentiviruses and myeloma cell transfection were previously described (Tiedemann et al., 2010).

### Antibodies

For immunoblots, antibodies sources were as follows: IRE1 (#3294, Cell Signaling Technology), ATF6 (#2940, Cell Signaling Technology), PERK (#3192, Cell Signaling Technology), ATF4 (#23760, Abcam), GADD34 (#125464, Abcam), DDIT3/CHOP (#27539, Abcam), DDIT4/REDD1 (#10638-1, Protein Tech), kappa (#AI3060, Vector Laboratories) or lambda (#AI3070, Vector Laboratories) immunoglobulin light chain, PAX5 (#12000, #109443; Abcam), BCL6 (Cell Signaling Technology), Blimp1 (#648202, BioLegend), or GAPDH (Ambion). For immunofluoresence, antibodies used included: mouse anti-XBP1S (#143F, Biolegend), Alexa Fluor 546 goat anti-mouse IgG (Invitrogen) and Alexa Fluor 647 goat anti-mouse IgG (Cell Signaling).

### RNAi screens

High throughput siRNA studies of >7,000 genes were conducted in KMS11 MM cells in the presence of titrated BTZ to identify synthetic lethal genes, as described (Tiedemann et al., 2012; Tiedemann et al., 2010; Zhu et al., 2011). To identify BTZ “rescue” genes or resistance mechanisms, genes were re-ranked by mean siRNA Bliss independence scores (Bliss, 1939) at cytotoxic bortezomib concentrations.

### Immunoblotting

Cells were washed in ice-cold phosphate-buffered saline and lysed in NP40 lysis buffer. Extracts were centrifuged and quantified by bicinchoninic acid assay (Pierce), and 10 μg/lane was separated by sodium dodecyl sulfate-polyacrylamide gel electrophoresis (SDS-PAGE). Standard and high MW proteins Ire1 (130 kDa), Atf6 (58 kDa), Perk (140 kDa), Gadd34 (73 kDa), Blimp1

(98 kDa) and Pax5 (42 kDa) were analyzed on 7.5% gels; lower MW proteins Ddit3 (Chop) (27 kDa) and IgL kappa or lambda (25 kDa) were analyzed on 15% gels; intermediate sized ATF4 (38kDa) was analyzed on either. Gapdh loading controls were assessed for each gel. Proteins were transferred to polyvinylidene fluoride membrane and probed with primary antibody(s). The 2˚ goat anti-rabbit or horse anti-mouse (Cell Signaling Technology) horseradish peroxidise-conjugated antibodies were used at a dilution of 1:10,000 and signal was detected using Amersham ECL Western Blotting Detection Reagents (GE Healthcare). Immunoblot bands were quantified by image densitometry (Image J).

**Lentivirus Production**

Lentiviruses were prepared in 293T packaging cells via transfection with a 3-plasmid system as previously described (Moffat et al., 2006; Naldini et al., 1996; Zufferey et al., 1997). Transfections were performed in 100 mm plates. Packaging cells were seeded at $3.5 \times 10^5$ cells per plate in IMDM/5% FCS 24 hrs before transfection and grown at 37˚C/5%$CO_2$. DNA for transfection was prepared by mixing 20 µg of shRNA/gene-encoded plasmid, 13.75 µg pSPAX, and 5.5 µg pMD2.G in 1.5 mL OptiMEM (Gibco). Lipofectamine 2000 (Invitrogen) 50 µL in 1.5 mL OptiMEM was combined with the DNA mix and allowed to complex for 20 min at room temperature before addition to the packaging cells. Cells were incubated overnight and the transfection reagent was subsequently removed and exchanged for IMDM/10%FBS. Lentiviral supernatants from 24 and 48 hours were pooled and lentivirus was frozen at -80˚C until use.

**Lentiviral Transductions**

All human myeloma cell line transductions were performed using 8 µg/mL of polybrene (Sigma). Transductions were conducted with lentivirus-containing supernatant diluted to 30-50% in IMDM/10% FCS over 16 hrs at 37˚C/5%$CO_2$.

**Cell viability – MTT-assay**

Cells were assayed in triplicate on 96-well plates. Following the indicated treatment viability was assessed by 3-(4,5-dimethylthiazol-2-yl)-2,5-

dimethyltetrazolium bromide (MTT) assay (Sigma) following the manufacturer's instructions. Results were plotted as the mean ± SEM (n=3).

**Cell viability – Flow cytometry**

Cells ($10^6$) were stained with Annexin V-FITC and propidium idodide at room temperature and fluorescence was determined by FACS (TACS AnnexinV-FITC Apoptosis Detection Kit; Trevigen kit 4830-250-K).

**Cell cycle analysis**

Cells ($10^6$) were prepared as described (Zhu et al., 2011), stained with 500μl of 50μg/ml propidium iodine (Sigma P4170) in 0.1% triton X100, 0.1% sodium citrate (hypotonic conditions) overnight at 4°C, assessed by FACS and analyzed by FlowJo.

**XBP1 plasmids and mutants**

XBP1 transcripts were PCR amplified from human XBP1u and XBP1s cDNA clones (OriGene) using 5'-GTTACCAGAATTCTGGTAATGGTGGTGGTGGCAG-3' (forward) and either 5'-ATTAAGGATCCTTAGTTCATTAATGGCTTCCAGCTT-3' or 5'-ATTAAGGATCCTCAAGGAAAAGGGCAACAGTA-3' (reverse) primers. *Bst*XI and *Bam*HI-digested products were cloned into pWPIs1 in NEB Turbo Competent E. *coli* (New England BioLabs). XBP1-L167I and P326R mutations were generated in pWPIS1-XBP1u and pWPIS1-XBP1s respectively, by PCR mutagenesis using 5'-GCTGAGTCCGCAGCAATCAGACTACGTGCACCTC-3' and 5'-GTGCACGTAGTCTGATTGCTGCGGACTCAGCAGA-3' primers for L167I; and 5'-ATCCAGCCACTGCCGAAAGCCATCTTCCTG-3' and 5'-CAGGAAGATGGCTTTCGGCAGTGGCTGGATG-3' primers for P326R.

**XBP1 splicing assay**

The XBP1 splicing assay has previously been described (Harding et al., 2005). RT-PCR was conducted using RNA isolated with TRIzol® (Invitrogen); 100ng was reverse transcribed from oligo dT priming and SuperScript III (Invitrogen). cDNA was quantified with a NanoDrop ND-1000 Spectrophotometer. PCR was performed on 3ug cDNA, denatured at 94°C for 4 min, using 5'-

AAACAGAGTAGCAGCTCAGACTGC-3' (XBP1.3S) and 5'-TCCCTTCTGGGTAGACCTCTGGGAG-3' (XBP1.12AS) primers, targeting positions 309 and 734 of GenBank sequence NM_005080, for 25 cycles (94˚C x 10s, 53˚C x 30s and 72˚C x 30s). Alternative primers, Fwd 5'-TTACGAGAGAAAACTCATGGC-3' and Rev 5'-GGGTCCAAGTTGTCCAGAATGC-3' were used in Figure 1; the alternative primers, sequences and PCR conditions were as described (Perez-Galan et al., 2011). Products were analyzed on a 3.5% agarose gel and visualized with a Gel Doc XR system (Bio-Rad).

**XBP1 target gene RT-PCR assay**

XBP1 target gene response to ectopic expression of XBP1u or XBP1s cDNAs from the EF1$\alpha$ promoter in pWPIs1 was determined by semi-quantitative RT-PCR. PCR conditions were identical to those described above for the XBP1 splicing assay. Products were resolved on a 1.5% agarose gel. Primers included DNAJB9 (CR533475.1) Fwd 5'-TGGTGGTTCCAGTAGACAAAGG-3', Rev 5'-CTTCGTTGAGTGACAGTCCTGC-3'; COX15 (AF044323.1) Fwd 5'-CAGCACCATCTCTGAAGTAGC-3', Rev 5'-CTGTCAACCTAGTTACTCCACC-3'; MGC29506 (plasma cell induced ER protein 1) (BC021275.2) Fwd 5'-CTGTCACTGCCACTGCTGC-3', Rev 5'-AGATTTTGCCACATCTGGTAAGCCA-3'; SEC61A1 (NM_013336.3) Fwd 5'-CTTAGTGTGCTGCCAGATTCC-3', Rev 5'-CCAGACGTGACAATAGGAGAG-3'; RHOQ (NM_012249) Fwd 5'-GTACCGGAACTTAAGGAATACG-3', Rev 5'-GCTAGTTTCTGTCCTTGTTCC-3'; and $\beta$-actin control (CAA25099.1) Fwd 5'-GCTCGTCGTCGACAACGGCTC-3' and Rev 5'-CAAACATGATCTGGGTCATCTTCTC-3'.

**Recapitulation of primary MM XBP1 mutations in MM tumor lines.**

Endogenous MM cell line XBP1 was silenced by stable LV integration expressing a 3'UTR-targeted shRNA. Control cells were simultaneously infected with NT shRNA lentivirus. XBP1 mRNA silencing was confirmed by semi-quantitiative PCR. Control and endogenous XBP1-silenced cells were then co-infected with second LV expression vectors (based upon an pWPIs1 backbone) delivering an exogenous XBP1 CDS without 3'UTR. Various pWPIs1-XBP1 vectors were used,

bearing XBP1s, XBP1u, XBP1u-L167I, XBP1s-P326R or no cDNA payload (empty); the desired mutations were generated by site directed mutagenesis. The treatment responses of patients that presented with primary MM XBP1 mutations were confirmed by personal communication (M Chapman).

**Gene Expression Data Resources**

Primary MM tumor profiles from pre-treatment MM patients enrolled on the APEX phase 3 trial (Study 039) of single agent bortezomib versus dexamethasone were obtained from NCBI GEO (http://www.ncbi.nlm.nih.gov/geo/)(GSE9782) (Mulligan et al., 2007). Three XBP1 signature gene sets were utilized. The first signature (XBP1_Staudt_SigDB) reflects XBP1 overexpression in B cells (Shaffer et al., 2006) and was obtained from http://lymphochip.nih.gov/signaturedb/; the second (V$XBP1_01) was derived from bioinformatic identification of all genes with promoters containing a conserved XBP1 motif and was obtained from the Broad MSigDB collection (c3) at http://www.broadinstitute.org/gsea/msigdb/index.jsp (Subramanian et al., 2005); the third, MM-specific, XBP1 signature (XBP1_MM), and a related IRE1 signature (IRE1_MM), were generated by shRNA knockdown of XBP1 or IRE1 in JJN3 and RPMI-8226 MM cells (data is available at NCBI GEO; GSE44968). Other lymphoid transcription factor signatures were obtained from http://lymphochip.nih.gov/signaturedb/. Gene expression profiles detailing B cell to plasma cell maturation were obtained from ArrayExpress (http://www.ebi.ac.uk/microarray-as/ae/) (E-MEXP-3034 and E-MEXP-2360)(Jourdan et al., 2011; Jourdan et al., 2009).

**Gene Expression Profiling of MM cell lines**

Total RNA was column purified with RNeasy MinElute Cleanup Kit (Qiagen). cDNA synthesis, cRNA preparation and hybridization to Affymetrix HG-U133 Plus 2.0 GeneChip microarrays (Affymetrix) was performed as recommended by the manufacturer. Median normalized gene expression profiles were analyzed using GeneSpring GX 12.1 (Agilent Technologies).

**GEP Analysis**

For primary MM tumor gene expression data (GSE9782)(Mulligan et al., 2007) from pre-treatment bone marrow aspirates from MM patients enrolled on the

APEX phase 3 trial (Study 039) of single agent bortezomib versus dexamethasone (Richardson et al., 2005), Affymetrix HG-U133A/B profiles were median normalized and censored to include only patients assigned to receive BTZ and whom experienced a CR or PD. The 44760 probesets were ranked by the ratio of the average expression intensity in BTZ CR versus PD tumors, ratio[CR/PD]. Lymphoid transcription factor target gene expression signatures for XBP1, IRF4, Blimp1, PAX5, MYC, STAT3, NF-κB and p53 (Shaffer et al., 2006), were superimposed on the GSE9782 probeset ranking.

**Gene Set Enrichment Analysis**

GSEA (Subramanian et al., 2005) was performed within GeneSpringGX. Three XBP1 signature genesets (XBP1_Staudt_SigDB, V$XBP1_01, and XBP1_MM) were utilized, as described above under gene expression data resources. The first (XBP1_Staudt_SigDB) reflects experimental XBP1 overexpression in B cells; the second (V$XBP1_01) was derived bioinformatically from the identification of genes with promoter regions around the transcription start site [-2kb,2kb] containing the conserved XBP1 motif NNGNTGACGTGKNNNWT; the third, MM-specific, XBP1 signature (XBP1_MM), and a related IRE1 signature (IRE1_MM), were generated by shRNA knockdown of XBP1 or IRE1 in JJN3 and RPMI-8226 MM cells and by comparison with NT shRNA treated control cells. Gene expression profiles on day 4 were captured on Affymetrix HG-U133 Plus 2.0 chipsets, as per the manufacturer's instructions and processed by RMA using quartile normalization. Genes with signal intensity falling below the 20%-ile in all four samples were filter as not expressed. For the MM-specific XBP1 or IRE1 gene sets, target genes were defined as expressed genes that decreased >2-fold with either shXBP1 or shIRE1 versus NT shRNA in one or both MM cell lines. All 4 XBP1 or IRE1 signature gene sets were tested for enrichment amongst genes preferentially expressed (fold-change >1.0) within BTZ-sensitive (CR) versus BTZ-resistant (PD) primary MM tumors (Mulligan et al., 2007). As profiling of individual tumors provides an aggregate of tumor subpopulations, wherein gene expression alterations within a cellular subpopulation may be reflected by only small changes in the overall profile, we included in this analysis all genes with any preferential expression (ratio>1.0) between BTZ response groups. As XBP1

and IRE1 gene sets were generated using HG-U133 Plus 2.0 technology while primary MM tumor data were captured using HG-U133A/B chipsets, IRE1, XBP1 and other transcription factor signature gene sets were censored prior to GSEA to remove U133A/B-irrelevant probe sets. For GSEA studies of maturation arrest in BTZ-resistant primary MM, plasma cell-lineage differentiation gene sets were derived that defined gene expression changes between memory B cells, activated $CD20^{high}CD38^{-}$ B-cells, activated $CD20^{low}CD38^{-}$ B-cells, $CD20^{-}CD38^{-}$ pre-plasmablasts, or $CD138^{-}CD38^{+}$ plasmablasts; and $CD138^{+}$ $CD38^{+}$plasma cells. Gene sets included probe sets whose average signal changed >2-fold between the nominated maturation stage and plasma cells; for each gene set the expression profile of mature plasma cells was a common denominator. Plasma cell-lineage maturation gene sets were tested by GSEA in primary MM BTZ-response groups.

**MM Patient Bone Marrow Samples**

Bone marrow samples from MM patients were obtained at the time of routine clinical procurement following informed consent. Cells were collected in heparinized tubes and processed by Ficoll-Plaque gradient. Tumor cells were enriched on a Beckman Coulter FACS Aria by FSC-SSC characteristics, negative selection for CD14, CD2 and 7AAD; and sorted in to subpopulations on the basis of CD38 and CD138 status. Sorted cells were cytospun onto microscope slides, stored desiccated at -80˚C, and further characterized by Immunofluorescence and FISH.

**Immunofluorescence**

Cytospin slides were thawed, fixed in 4% paraformaldehyde, permeabilized with 0.5% Triton X-100, stained with primary antibody for 2 hours and a fluorochrome-conjugated secondary antibody for 1 hour at room temperature and mounted in Vectashield with DAPI (Vector Laboratories, Inc.). Images were generated with a Zeiss Axio Imager M1 microscope using AxioVision (Carl Zeiss AG) or Isis (MetaSystems Group, Inc.) acquisition software. antibodies. XBP1s protein expression was categorized into positive (+), negative (-) or weak (wk) using the

scale shown in supplemental Fig S3. A similar scale was utilized for assessing Ddit3 (Chop) protein expression.

**Fluorescence in situ Hybridization (FISH)**

Cytospin slides were fixed in ice-cold 3:1 methanol/acetic acid, incubated in 2X SSC for 30 min at 37$^{o}$C, dehydrated in a series of ethanol washes and hybridized with Vysis LSI (Abbott Molecular) or Cytocell Aquarius DNA Probes according to the manufacturer's instructions. Probe sets included Vysis LSI IGH/CCND1 (14q32:11q13) and LSI IGH/FGFR3(14q32:4p16) Dual Color translocation probes, Vysis LSI D5S23, D5S721 SGn/CEP 9 SA/CEP 15 SO Probes and Cytocell Aquarius CKS1B/CDKN2C(p18) Amplification/Deletion Probes (1q21/1p32.3). 100 cells or more from each slide were scored. The background rate for each set of FISH probes was determined by counting >200 cells from pooled bone marrow from 5 healthy male donors.

**Combined Immunofluorescence and FISH (ImmunoFISH)**

Cytospin slides were fixed, permeabilized and stained for immunofluorescence as described above and the X,Y-coordinates of cells were recorded during image acquisition. Cover slips were then removed and cells subjected to protease treatment using 0.005% pepsin in 0.01N HCl for 10 min at 37$^{o}$C. Cells were then washed in PBS, fixed in 1% formaldehyde for 5 min at room temperature, washed in PBS, and dehydrated by ethanol washes for FISH probe hybridization as described above. FISH images were acquired at the X,Y coordinates corresponding to IF images. Studies assessing Xbp1s, CD20, CD27 or Ddit3 (Chop) protein expression in progenitor subpopulations were restricted to cells showing a clonal FISH abnormality specific to the tumor examined.

## SUPPLEMENTAL REFERENCES


Bliss, C. I. (1939). The toxicity of poisons applied jointly. Ann Appl Biol *26*, 585–615.

Chen, M., Gutierrez, G. J., and Ronai, Z. A. (2011). Ubiquitin-recognition protein Ufd1 couples the endoplasmic reticulum (ER) stress response to cell cycle control. Proc Natl Acad Sci U S A *108*, 9119-9124.

Dombroski, B. A., Nayak, R. R., Ewens, K. G., Ankener, W., Cheung, V. G., and Spielman, R. S. (2010). Gene expression and genetic variation in response to endoplasmic reticulum stress in human cells. Am J Hum Genet *86*, 719-729.

Harding, H. P., Zhang, Y., Khersonsky, S., Marciniak, S., Scheuner, D., Kaufman, R. J., Javitt, N., Chang, Y. T., and Ron, D. (2005). Bioactive small molecules reveal antagonism between the integrated stress response and sterol-regulated gene expression. Cell Metab *2*, 361-371.

Jin, H. O., Seo, S. K., Woo, S. H., Kim, E. S., Lee, H. C., Yoo, D. H., An, S., Choe, T. B., Lee, S. J., Hong, S. I*., et al.* (2009). Activating transcription factor 4 and CCAAT/enhancer-binding protein-beta negatively regulate the mammalian target of rapamycin via Redd1 expression in response to oxidative and endoplasmic reticulum stress. Free Radic Biol Med *46*, 1158-1167.

Jourdan, M., Caraux, A., De Vos, J., Fiol, G., Larroque, M., Cognot, C., Bret, C., Duperray, C., Hose, D., and Klein, B. (2009). An in vitro model of differentiation of memory B cells into plasmablasts and plasma cells including detailed phenotypic and molecular characterization. Blood *114*, 5173-5181.

Moffat, J., Grueneberg, D. A., Yang, X., Kim, S. Y., Kloepfer, A. M., Hinkle, G., Piqani, B., Eisenhaure, T. M., Luo, B., Grenier, J. K*., et al.* (2006). A lentiviral RNAi library for human and mouse genes applied to an arrayed viral high-content screen. Cell *124*, 1283-1298.

Naldini, L., Blomer, U., Gallay, P., Ory, D., Mulligan, R., Gage, F. H., Verma, I. M., and Trono, D. (1996). In vivo gene delivery and stable transduction of nondividing cells by a lentiviral vector. Science *272*, 263-267.

Prenzel, T., Begus-Nahrmann, Y., Kramer, F., Hennion, M., Hsu, C., Gorsler, T., Hintermair, C., Eick, D., Kremmer, E., Simons, M*., et al.* (2011). Estrogen-dependent gene transcription in human breast cancer cells relies upon proteasome-dependent monoubiquitination of histone H2B. Cancer Res *71*, 5739-5753.

Subramanian, A., Tamayo, P., Mootha, V. K., Mukherjee, S., Ebert, B. L., Gillette, M. A., Paulovich, A., Pomeroy, S. L., Golub, T. R., Lander, E. S., and Mesirov, J. P. (2005). Gene set enrichment analysis: a knowledge-based approach for interpreting genome-wide expression profiles. Proc Natl Acad Sci U S A *102*, 15545-15550.

Zufferey, R., Nagy, D., Mandel, R. J., Naldini, L., and Trono, D. (1997). Multiply attenuated lentiviral vector achieves efficient gene delivery in vivo. Nat Biotechnol *15*, 871-875.